

ARTICLES

Irradiation-induced transformation of graphite to diamond: A quantitative study

Michael Zaiser, Yuliya Lyutovich, and Florian Banhart

Max-Planck-Institut für Metallforschung, D-70569 Stuttgart, Germany

(Received 31 August 1999; revised manuscript received 13 January 2000)

High-energetic particle irradiation of carbon structures containing a graphite-diamond interface can lead to low-pressure diamond growth. A theoretical model predicting irradiation-induced diamond growth has been presented in a previous paper [Zaiser and Banhart, *Phys. Rev. Lett.* **79**, 3680 (1997)]. In the present study, a quantitative experimental investigation of the phase transformation kinetics during electron irradiation in a high-voltage electron microscope is reported. Phase stability and phase transformation velocities are determined as functions of temperature, irradiation energy, and intensity. Experimentally determined phase boundaries and growth velocities are interpreted in terms of the theoretical model.

I. INTRODUCTION

The transformation of graphite to diamond has been a challenge since its first successful undertaking in the 1950s.^{1,2} Until recently, it has been assumed that high pressure is generally needed to carry out this transformation. Graphite is the stable phase of carbon at low pressure, and a kinetic route from graphite to diamond at low pressure has not been discovered. The only way of producing diamond at low pressure has been the immediate nucleation of diamond from the gas phase where the formation of the more stable phase, graphite, is kinetically hindered.³ The reversal of phase stability is, at moderate temperatures, not obtained until pressures of a few gigapascals are exceeded.⁴ However, when graphite is exposed to increasing pressure, the kinetic barrier between the two phases still prevents the direct transformation at the equilibrium phase boundary so that either extreme pressures, high temperatures and pressures, or, technically most important, the use of catalysts is necessary for the transformation of reasonable amounts of graphite to diamond.

In a recent study, graphitic carbon onions have been irradiated with an intense high-energetic electron beam at high temperature.⁵ It has been shown that under these conditions, carbon onions undergo heavy self-compression^{5,6} which leads to the nucleation of diamond crystals in their cores. Surprisingly, the diamond nuclei were seen to grow under further irradiation until the graphitic onions had wholly transformed to diamonds.⁷ This phenomenon is remarkable because the late stages of this transformation occur under low or even vanishing pressure. Starting out from this observation, a theoretical model was developed⁸ which predicts that irradiation with energetic particles may, in a certain regime of irradiation temperatures and intensities, reverse phase stability in the graphite-diamond system. In a follow-up study, it was confirmed experimentally that the irradiation-induced transformation of graphite to diamond is feasible on a general scale,⁹ i.e., not restricted to carbon onions with their particular geometry.

In the present paper, a detailed quantitative study of the nonequilibrium phase diagram of carbon under irradiation is presented. The phase boundaries and transformation velocities are investigated as functions of temperature, irradiation intensity, and energy of the irradiating particles (here we restrict our experiments and considerations to high-energetic electrons). The experiments are carried out by *in situ* transmission electron microscopy (TEM) where irradiation and atomic-scale imaging are done at the same time and in the same instrument. To interpret the experimental findings, we use a modified version of the model by Zaiser and Banhart.⁸ The theoretical treatment is based on the master equation approach towards phase evolution kinetics under irradiation worked out by Bellon and Martin.¹⁰ This is generalized to an incoherent phase transformation involving the motion of an interface between two phases. The approach leads to the definition of a nonequilibrium effective free energy which governs phase stability under irradiation and yields quantitative predictions of the interface velocity which can be directly compared to the experimental observations.

II. EXPERIMENT

The irradiation studies were carried out by using a specimen containing a graphite-diamond interface which was investigated in a TEM at high resolution. As in a previous study,⁹ a chemical vapor deposition (CVD) diamond film was thinned by Ar⁺ ion sputtering so as to be transparent to electrons. After ion sputtering and annealing at temperatures above 1000 K the diamond specimen had a graphite layer of up to 150 nm in thickness on the diamond surface. The interface between the diamond crystal and the graphite surface layer was imaged and irradiated in high-resolution TEM's. Instruments operating at 1250 kV (Jeol ARM 1250) and at 80–400 kV (Jeol 4000FX) were used. The irradiation was carried out at electron energies of 150, 200, 400, and 1250 keV. Heating specimen stages enabled us to vary the specimen temperature in the range from 290–1270 K. The beam current density was varied in the range from 5–240 A/cm².

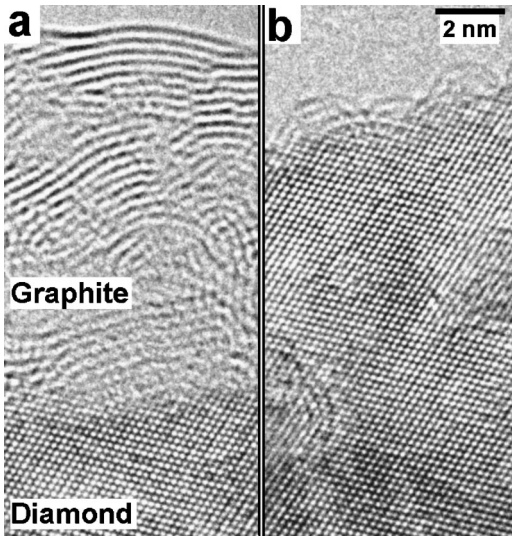


FIG. 1. Atomic resolution electron micrographs of a graphite-diamond interface; (a) before irradiation, (b) after 220 min of 1250-keV electron irradiation at $T=1000$ K with a current density of 30 A/cm². Under these conditions, diamond grows at the expense of graphite.

The beam current was measured by using Faraday cups (with a slight inaccuracy due to the escape of an unknown fraction of backscattered and secondary electrons).

During the irradiation, lattice images showing the location of the interface were recorded on photographic film or by a slow-scan charge-coupled device (CCD) camera. The velocity of the interface, moving either towards the graphite or the diamond region, depending on whether graphite or diamond grew, could hence be measured.

Figure 1 illustrates the initial and final stage of the transformation of a graphite surface layer to diamond under electron irradiation. After 220 min irradiation with 1250-keV electrons at 1000 K and a beam intensity of 30 A/cm², the graphite layer with an initial thickness of 7 nm has completely transformed to diamond.

III. THEORY

We consider a model system consisting of N carbon atoms and assume that N_D of these atoms are arranged on the sites of a diamond lattice, while the remaining $(1-N_D)$ atoms form a graphite lattice, and that both phases are separated by an atomically sharp interface. Thermodynamically, the system is characterized by a Gibbs free energy $G(N_D) \approx N_D G_D + (1-N_D)G_G$, where G_D and G_G are the Gibbs free energies of carbon atoms in the bulk diamond and graphite phases, respectively. (Since the atomic volumes of diamond and graphite are quite different, the volume of the system is not constant when N_D changes. Hence one must use the Gibbs free energy G rather than the Helmholtz free energy F for characterizing the thermodynamic state of the system.) Note that we may always take N sufficiently large such that the contribution of the interface to the total free energy can be neglected. The free energies are assumed the same as for an unirradiated crystal, i.e., we neglect damage accumulation (cf. below). Hence the Gibbs free energy depends for a given system size on the ratio N_D/N only, which

we may consider as the order parameter of the graphite-to-diamond transition.

Under irradiation, two different kinds of processes may contribute to an exchange of atoms through the interface between both phases:

(i) Carbon atoms may pass from diamond to graphite and vice versa through processes which are governed by thermal activation only. This is expressed in terms of net thermal jump rates across the interface $\Gamma_{\text{th}}^{\text{G-D}}$ (from graphite to diamond) and $\Gamma_{\text{th}}^{\text{D-G}}$ (from diamond to graphite). Due to local thermal equilibrium, these rates must obey the relationship

$$\frac{\Gamma_{\text{th}}^{\text{G-D}}}{\Gamma_{\text{th}}^{\text{D-G}}} = \exp\left[-\frac{\Delta G}{k_B T}\right], \quad (1)$$

where $\Delta G = G_D - G_G$ is the Gibbs free energy difference between diamond and graphite, k_B is Boltzmann's constant, and T temperature. Introducing the total rate $\nu_{\text{th}} = \Gamma_{\text{th}}^{\text{G-D}} + \Gamma_{\text{th}}^{\text{D-G}}$ of thermally activated jumps across the interface, one may write

$$\Gamma_{\text{th}}^{\text{D-G}} = p^{\text{D-G}} \nu_{\text{th}}, \quad \Gamma_{\text{th}}^{\text{G-D}} = p^{\text{G-D}} \nu_{\text{th}}, \quad (2)$$

where the probabilities $p^{\text{D-G}}$ and $p^{\text{G-D}} = (1-p^{\text{D-G}})$ are given by

$$p^{\text{D-G}} = \frac{1}{1 + \exp\left[-\frac{\Delta G}{k_B T}\right]}, \quad (3a)$$

$$p^{\text{G-D}} = \frac{\exp\left[-\frac{\Delta G}{k_B T}\right]}{1 + \exp\left[-\frac{\Delta G}{k_B T}\right]}. \quad (3b)$$

Due to the thermodynamic stability of graphite ($\Delta G > 0$), $p^{\text{G-D}}$ is smaller than $p^{\text{D-G}}$ for all T . The total rate ν_{th} of ‘‘thermal’’ jumps of atoms across the interface is assumed to be governed by an Arrhenius law with an effective activation energy G_{th} ,

$$\nu_{\text{th}} = \nu_0 \exp\left[-\frac{G_{\text{th}}}{k_B T}\right], \quad (4)$$

where $\nu_0 \approx 10^{13}$ s⁻¹ is an attempt frequency of the order of the Debye frequency.

(ii) In addition to the thermally activated jumps across the interface, under particle irradiation nonequilibrium processes involving the ballistic displacement of atoms may lead to an exchange of atoms between the two phases. We conceive such ‘‘ballistic’’ jumps as two-step processes: In a first step, collision with an incident particle leads to the displacement of a carbon atom from a diamond or graphite lattice site to the interface (production of an interface interstitial). In a second step, the interface interstitial relaxes to a vacant interface or bulk lattice site.

The displacement process can be characterized by the displacement threshold energy T_d , i.e., the minimum energy that must be transferred to an atom in order to produce a stable vacancy-interstitial pair. In crystalline structures, T_d in general depends on the direction of the displacement. In the

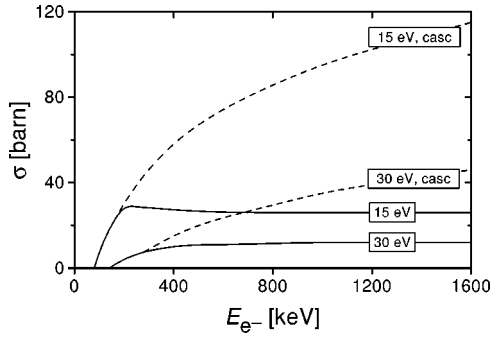


FIG. 2. Cross section for the displacement of carbon atoms by electrons as a function of the electron energy for displacement threshold energies of 15 and 30 eV. The full lines pertain to single atom displacements, the dashed lines are corrected for the effect of cascades leading to the production of multiple defects.

present work, we use isotropic effective displacement thresholds $T_{\text{d,eff}}^{\text{X}}$ ($\text{X}=\text{D}$ for diamond and $\text{X}=\text{G}$ for graphite) obtained from bulk radiation damage experiments. There is a significant scatter in the literature data: While in earlier studies (for compilation, see the review by Thrower and Mayer¹¹) threshold energies between 24 and 48 eV have been reported for graphite, recent experiments yielded lower values ranging between 12 (Ref. 12) and 15–20 eV.¹³ For diamond, displacement threshold energies compiled in the review by Banhart¹⁴ range between 30 and 48 eV. In the present work, we use the values $T_{\text{eff}}^{\text{G}}=15$ eV and $T_{\text{eff}}^{\text{D}}=30$ eV for graphite and diamond, respectively. (Since we expect displacement threshold energies close to the diamond-graphite interface to be somewhat lower than in bulk crystals, we use values corresponding to the lower end of the data range reported in the literature.) As a most important feature characterizing the behavior of irradiated carbon it is noted that graphite, where atoms can be displaced easily in the direction of the c axis,¹⁴ exhibits a lower displacement threshold than diamond. This asymmetry leads to preferential damage of graphite and is the main reason why the far-from-equilibrium “excitation” by irradiation may drive a graphite-to-diamond transformation.

From the displacement threshold energies, displacement cross sections pertaining to different electron energies can be obtained using the theory of Mott scattering. In our calculations we have used an algorithm developed by Hohenstein *et al.*¹⁵ In Fig. 2, cross sections σ for the displacement of carbon atoms by electrons are given as a function of the electron energy for threshold energies of 15 eV (graphite) and 30 eV (diamond). While the full curves pertain to single displacements, the dashed curves are corrected for cascade effects, accounting for the fact that at high transferred energies the displaced atom may cause secondary displacements, leading to the formation of more than one stable defect.

After an interface interstitial has been produced, there is a large number of nearby interface sites where it may recombine, i.e., its relaxation requires only a few diffusional jumps. In the range of temperatures and displacement rates relevant to the present study, this implies that the relaxation process is fast as compared to the time between two atomic displacements [in diamond, interstitials are mobile already below room temperature² while in graphite annealing studies indicate that interstitials reach a jump frequency of about

1 s^{-1} at 320 K (Ref. 14)], and that accumulation of interface interstitials can be neglected. Hence the net ballistic jump rates from graphite to diamond and vice versa can be written as

$$\Gamma_{\text{irr}}^{\text{G-D}} = \sigma_{\text{G}} \Phi p^{\text{I-D}}, \quad \Gamma_{\text{irr}}^{\text{D-G}} = \sigma_{\text{D}} \Phi p^{\text{I-G}}, \quad (5)$$

where Φ is the irradiation flux, σ_{G} and σ_{D} are the respective cross sections for displacement of atoms from graphite and diamond lattice sites, and $p^{\text{I-D}}$ and $p^{\text{I-G}}$ denote the average probabilities for an interface interstitial to relax to a diamond or graphite lattice site, respectively.

These probabilities can again be formulated within a thermodynamic framework. When doing so, it is important to note that the relaxation probabilities do not depend on the free energy of the final state (graphite or diamond lattice atom) but on the effective energy barriers required to reach this from the irradiation-produced metastable initial state (interface interstitial). In this respect, the treatment in the previous paper⁸ was erroneous. In the present work, we characterize the relaxation processes by effective energy barriers $G^{\text{I-D}}$ and $G^{\text{I-G}}$ for the relaxation of interface interstitials to diamond and graphite lattice sites, respectively. Then the relaxation probabilities may be expressed as

$$p^{\text{I-G}} = \frac{1}{1 + \exp\left[-\frac{\Delta G^{\text{I}}}{k_{\text{B}}T}\right]}, \quad (6a)$$

$$p^{\text{I-D}} = \frac{\exp\left[-\frac{\Delta G^{\text{I}}}{k_{\text{B}}T}\right]}{1 + \exp\left[-\frac{\Delta G^{\text{I}}}{k_{\text{B}}T}\right]}, \quad (6b)$$

where $\Delta G^{\text{I}} = G^{\text{I-D}} - G^{\text{I-G}}$ is the difference in the effective energy barriers for relaxation of interface interstitials to diamond or graphite lattice sites (relaxation barrier asymmetry).

Taking into account both ballistic and thermal jump processes, our model system can be characterized by a master equation for the probability $P(N_{\text{D}})$ of finding N_{D} atoms on diamond lattice sites. This is given by

$$\begin{aligned} \frac{1}{N_{\text{I}}} \frac{\partial P(N_{\text{D}})}{\partial t} = & \Gamma_{\text{tot}}^{\text{G-D}} P(N_{\text{D}} - 1) + \Gamma_{\text{tot}}^{\text{D-G}} P(N_{\text{D}} + 1) \\ & - [\Gamma_{\text{tot}}^{\text{D-G}} + \Gamma_{\text{tot}}^{\text{G-D}}] P(N_{\text{D}}), \end{aligned} \quad (7)$$

where the total jump rates are $\Gamma_{\text{tot}}^{\text{X-Y}} = \Gamma_{\text{th}}^{\text{X-Y}} + \Gamma_{\text{irr}}^{\text{X-Y}}$ ($\text{X-Y} = \text{D-G}$ or G-D), all rates are understood as average jump rates per interface atom, and N_{I} is the number of such atoms.

A. Nonequilibrium effective free energy

It is instructive to consider the solution of the master equation (7) under steady-state conditions. This is obtained by requiring detailed balance, $\Gamma_{\text{tot}}^{\text{G-D}} P(N_{\text{D}} - 1) = \Gamma_{\text{tot}}^{\text{D-G}} P(N_{\text{D}})$. It readily follows that the steady-state solution of Eq. (7) is

$$P(N_{\text{D}}) = \mathcal{N} \exp[-\Psi(N_{\text{D}})], \quad (8)$$

$$\Psi(N_D) = \Psi(0) + \sum_0^{N_D-1} \ln \frac{\Gamma_{\text{tot}}^{D-G}}{\Gamma_{\text{tot}}^{G-D}}. \quad (9)$$

Here \mathcal{N} is a normalization constant chosen such that $\sum_{N_D=0}^N P(N_D) = 1$.

In the expression (8), the ‘‘stochastic potential’’ Ψ of the nonequilibrium system plays much the same role as the thermodynamic potential divided by $k_B T$ for an equilibrium system. This analogy leads us to the concept of a nonequilibrium ‘‘effective free energy’’ G_{eff} which governs phase stability under irradiation. We define the difference in the effective free energies per atom on the diamond and graphite lattice as

$$\Delta G_{\text{eff}} = k_B T [\Psi(N) - \Psi(0)]/N. \quad (10)$$

Using Eqs. (2)–(5), (9), and (10) one finds

$$\Delta G_{\text{eff}} = \Delta G - k_B T \ln \left[\frac{1 + \frac{\Phi \sigma_G}{\nu_{\text{th}}} \frac{p^{I-D}}{p^{G-D}}}{1 + \frac{\Phi \sigma_D}{\nu_{\text{th}}} \frac{p^{I-G}}{p^{D-G}}} \right], \quad (11)$$

while according to Eq. (8) the probability distribution is $P(N_D) = \mathcal{N} \exp[-N_D \Delta G_{\text{eff}}/k_B T]$.

In the absence of irradiation ($\Phi=0$) as well as at high temperatures ($\nu_{\text{th}} \gg \Phi \sigma_D, \Phi \sigma_G$) where thermal exchange of atoms across the interface prevails, ΔG_{eff} reduces to the Gibbs free-energy difference ΔG , i.e., the system behaves as in thermal equilibrium. On the other hand, during irradiation at not too high temperatures, ballistic jumps may become predominant ($\nu_{\text{th}} \ll \sigma_D \Phi, \sigma_G \Phi$). In this case the second term on the right-hand side of Eq. (11) may lead to a reduction of the nonequilibrium effective free energy of the atoms in the diamond lattice and eventually to a negative effective free-energy difference ΔG_{eff} between diamond and graphite, indicating reversal of phase stability under irradiation. In the low-temperature regime where thermal jumps may be neglected ($\nu_{\text{th}} \rightarrow 0$), the condition for phase stability reversal ($\Delta G_{\text{eff}} \leq 0$) according to Eqs. (3), (6), and (11) is approximately

$$\ln \left[\frac{\sigma_G}{\sigma_D} \right] \geq \frac{\Delta G^I}{k_B T}. \quad (12)$$

In this regime, the qualitative behavior of the system depends on the sign of the relaxation barrier asymmetry ΔG^I . [In the previous paper,⁸ this has been equated to the difference ΔG in bulk free energies. In the present paper, we determine ΔG^I from the experimental nonequilibrium phase diagram (Sec. IV).] When interface interstitials recombine preferentially on diamond sites, $\Delta G^I < 0$, Eq. (12) is always fulfilled (i.e., phase stability is reversed) since $\sigma_G > \sigma_D$. If, on the other hand, recombination takes place preferentially on graphite sites ($\Delta G^I > 0$), Eq. (12) defines a lower critical temperature T_1 for phase stability reversal. Below T_1 , jumps from diamond to graphite prevail ($\Gamma_{\text{irr}}^{D-G} > \Gamma_{\text{irr}}^{G-D}$) in spite of the larger displacement cross section in graphite since $p^{I-D} \ll p^{I-G}$. Only above T_1 the probability for relaxation to a diamond site is sufficiently large such that phase stability is

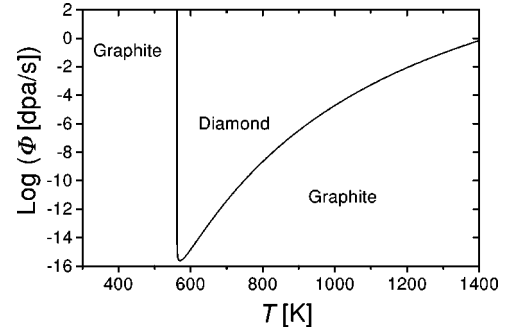


FIG. 3. Nonequilibrium phase diagram (displacement rate vs temperature) of the diamond-graphite system under electron irradiation; parameters: $\sigma_G=104$ b, $\sigma_D=40$ b, $\Delta G^I=0.047$ eV, $G_{\text{th}}=3.2$ eV; the displacement rate refers to the graphite phase.

reversed. Note that T_1 depends on the ratio of the displacement cross sections in graphite and diamond and on the relaxation barrier asymmetry ΔG^I , but not on the irradiation intensity Φ : Since only irradiation-induced processes are relevant at low temperatures, in this regime all rates are proportional to Φ . Hence a change in irradiation intensity modifies the velocity but not the direction of the transformation.

At high temperatures the ‘‘thermal’’ jump rates ν_{th} can no longer be neglected. Above an upper critical temperature T_2 where the effects of thermal and ballistic jumps balance each other, thermal jumps lead to a net transport of matter from diamond to graphite and make graphite again the stable phase. This upper critical temperature decreases with decreasing displacement rate. At a lower critical displacement rate, the upper and lower critical temperature branches merge, and below this critical displacement rate graphite is for all temperatures the stable phase.

This behavior is illustrated in Fig. 3 which shows a nonequilibrium phase diagram calculated for irradiation with 1250-keV electrons. Displacement cross sections have been determined using the parameters $T_{\text{eff}}^G=15$ eV and $T_{\text{eff}}^D=30$ eV and accounting for cascade effects (cf. dashed curves in Fig. 2). This yielded $\sigma_G=10.4 \times 10^{-27}$ m² and $\sigma_D=4 \times 10^{-27}$ m². The difference $\Delta G = \Delta G(p, T)$ in the (equilibrium) Gibbs free energies of graphite and diamond was taken from literature data,¹⁶ and the parameters $\Delta G^I=0.047$ eV and $G_{\text{th}}=3.2$ eV were assumed. (For determination of these parameters, see Sec. IV.) In Fig. 3, phase boundaries are given in terms of temperature and irradiation intensity, where the latter is characterized by the rate of atomic displacements in graphite. [The unit ‘‘dpa’’ (displacements per atom) is the irradiation dose required to displace, on the average, each atom once from its lattice site.]

B. Phase transformation velocity

While the steady-state solution of the master equation (7) yields information about phase stability in terms of an effective free energy of the nonequilibrium system, this equation may be also used to study the time-dependent behavior, i.e., the phase transformation dynamics.

We consider the transient behavior during diamond growth, when both $P(0)$ and $P(N)$ can be assumed negligi-

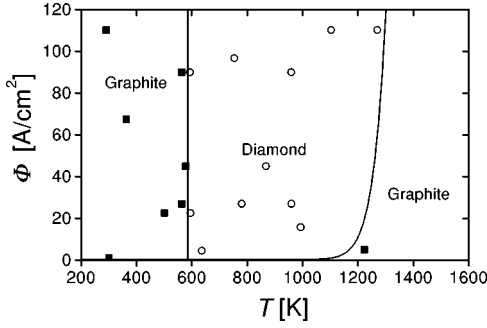


FIG. 4. Experimentally determined nonequilibrium phase diagram (irradiation intensity vs temperature) for irradiation with 1250-keV electrons; open circles: diamond growth ($v_i > 0$), black squares: graphite growth; full line: theoretical curve calculated for the same parameters as in Fig. 3.

bly small. Then from Eq. (7) the evolution of the average number of atoms on diamond lattice sites, $\langle N_D \rangle = \sum_0^N N_D P(N_D)$, follows as

$$\partial_t \langle N_D \rangle = N_i (\Gamma_{\text{tot}}^{\text{G-D}} - \Gamma_{\text{tot}}^{\text{D-G}}). \quad (13)$$

From this we obtain the average velocity of the diamond-graphite interface in a coordinate system attached to the diamond lattice, $v_i = b(\Gamma_{\text{tot}}^{\text{G-D}} - \Gamma_{\text{tot}}^{\text{D-G}})$ where $b = V_D^{1/3}$ and V_D is the atomic volume in diamond. Positive v_i indicate diamond growth. At the phase boundary where $\Delta G_{\text{eff}} = 0$, also v_i goes through zero and becomes negative for $T < T_1$ and $T > T_2$. We note that the same mechanism (ballistic creation + thermal relaxation of interface interstitials) which for $T_1 < T < T_2$ leads to diamond growth, at low temperatures promotes the transformation of diamond to graphite which in the absence of irradiation would be kinetically frozen in because of the negligibly small thermal jump rates.

Using Eqs. (2)–(7), we get an explicit expression for the interface velocity,

$$v_i = \Phi b \frac{\sigma_G \exp\left(-\frac{\Delta G^{\text{I}}}{k_B T}\right) - \sigma_D}{1 + \exp\left(-\frac{\Delta G^{\text{I}}}{k_B T}\right)} - \nu_0 b \exp\left(-\frac{\Delta G^{\text{I}}}{k_B T}\right) \frac{1 - \exp\left(-\frac{\Delta G}{k_B T}\right)}{1 + \exp\left(-\frac{\Delta G}{k_B T}\right)}. \quad (14)$$

For temperatures well below T_2 , the first term on the right-hand side of this equation predominates. In this regime, the velocity of the irradiation-driven phase transformation is directly proportional to the irradiation intensity, irrespective of the direction of the transformation.

IV. RESULTS AND DISCUSSION

For irradiation with 1250-keV electrons, phase transformation velocities have been determined for various temperatures and irradiation intensities. Figure 4 gives a nonequilibrium phase diagram for 1250-keV electron irradiation and zero pressure in terms of irradiation intensity vs temperature.

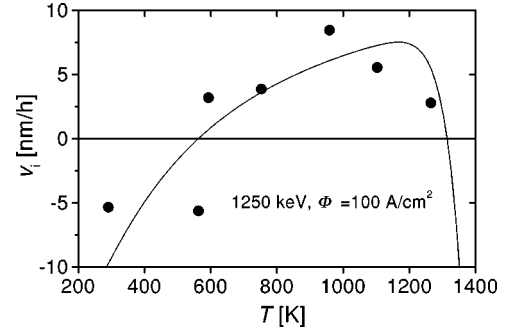


FIG. 5. Velocity of the diamond-graphite transformation as a function of temperature for irradiation with 1250-keV electrons and a beam intensity of 100 A/cm²; full line: theoretical curve according to Eq. (14), parameters as in Figs. 3 and 4.

The open circles denote those parameters where irradiation-induced diamond growth has been observed, while black squares indicate graphite growth. Note that the irradiation intensity is given in linear scale, as opposed to the logarithmic scale of Fig. 3. Diamond growth is observed only above a critical temperature $T_1 \approx 570$ K. According to the model presented in the previous section, the observation of a lower critical temperature is interpreted in terms of preferential recombination of irradiation-induced interface interstitials on graphite sites (positive relaxation barrier asymmetry ΔG^{I}). As predicted by the theory, T_1 does not depend on irradiation intensity. From T_1 the relaxation barrier asymmetry ΔG^{I} is obtained using Eq. (12). With $\sigma_G = 10.4 \times 10^{-27}$ m² and $\sigma_D = 4 \times 10^{-27}$ m² (displacement cross sections for 1250-keV electrons and $T_G^{\text{eff}} = 15$ eV, $T_D^{\text{eff}} = 30$ eV, cf. above) one obtains $\Delta G^{\text{I}} = 0.047$ eV. At high temperatures, diamond growth depends on both temperature and irradiation intensity: While for an irradiation intensity of 100 A/cm² diamond growth was observed up to 1270 K, for a much lower intensity of about 5 A/cm² the graphite layer was observed to grow at 1223 K. Temperatures above 1270 K were not accessible with the specimen stage used in this study. The available high-temperature data are consistent with a characteristic activation enthalpy $G_{\text{th}} = 3.2 \pm 0.1$ eV.

Measured phase transformation velocities (mean velocities of the diamond-graphite interface) are given in Fig. 5 for 1250 keV electron irradiation with an intensity of 100 A/cm² and various irradiation temperatures. These velocities were determined during the initial stages of the transformation when no systematic dependency of the phase transformation velocity on the orientation of the interface with respect to the diamond or graphite lattices was observed. (During the very last stages of the transformation of the graphite layer, on the other hand, curved onionlike structures emerged within the residual graphitic material, and diamond was found to grow preferentially into these structures.) The experimental data are well represented by the theoretical curve calculated from Eq. (14) using the parameters $\Delta G^{\text{I}} = 0.047$ eV and $G_{\text{th}} = 3.2$ eV as determined from the nonequilibrium phase diagram. For irradiation with 400-keV electrons, phase transformation velocities have been measured as a function of temperature for an irradiation intensity of 150 A/cm² (Fig. 6). Displacement cross sections for this electron energy have been determined in a similar manner as for 1250-keV electrons, yielding $\sigma_G = 5.8 \times 10^{-27}$ m² and

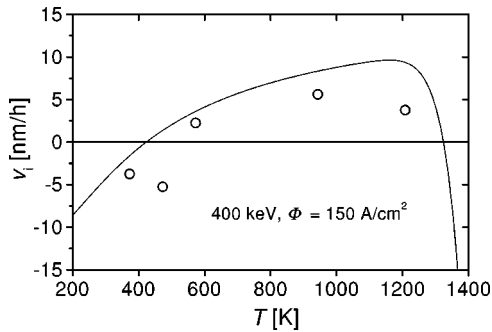


FIG. 6. Velocity of the diamond-graphite transformation as a function of temperature for irradiation with 400-keV electrons and a beam intensity of 150 A/cm²; full line: theoretical curve calculated with $\sigma_G=58$ b and $\sigma_D=15$ b (displacement cross sections for 400-keV electrons, cf. Fig. 2); other parameters as in Figs. 3–5.

$\sigma_D=1.5 \times 10^{-27}$ m². Phase transformation velocities calculated with these cross sections (full line in Fig. 6) are again in good agreement with the experimental data.

To assess the dependency of phase transformation velocity on irradiation intensity, measurements performed under irradiation with 1250-keV electrons at various intensities have been compiled in Fig. 7. All velocities have been scaled by the respective irradiation intensities times the atomic volume in diamond. (For illustration: With $V_{at}=5.67 \times 10^{-30}$ m⁻³ and $\Phi=100$ A/cm² (i.e., 6.25×10^{24} e⁻/[m²s]), a scaled velocity of 5×10^{-8} corresponds to a dimensional value of about 6 nm/h.) The scaled velocities are compared with the predictions of the theoretical model (full and dashed lines in Fig. 7). According to the model, at low and intermediate temperatures the transformation velocities are expected proportional to the irradiation intensity, i.e., the scaled velocities are intensity independent. Close to the upper critical temperature, on the other hand, one expects a significant dependence of the scaled velocities on irradiation intensity. Both predictions are consistent with the experimental data.

The experimental observations compiled in the present section are in good agreement with the predictions of the theoretical model developed in Sec. II:

- Irradiation-induced diamond growth takes place in an intermediate temperature regime.
- The upper critical temperature increases with increasing irradiation intensity, while the lower critical temperature is intensity independent.
- At low and intermediate temperatures, the phase transformation velocity is proportional to the irradiation intensity.

Irradiation-induced diamond growth is interpreted in terms of preferential damage of graphite (lower displacement threshold energy), while the observation of a lower critical temperature is related to the preferential recombination of interface interstitials on graphite sites. Using effective displacement threshold energies $T_{d,eff}^G=15$ eV for graphite and $T_{d,eff}^D=30$ eV for diamond, an activation energy $G_{th}=3.2$ eV and a relaxation barrier asymmetry $\Delta G^I=0.047$ eV, the nonequilibrium phase diagram observed for 1250 keV electron irradiation could be reproduced, and quantitative agreement between theoretically calculated and

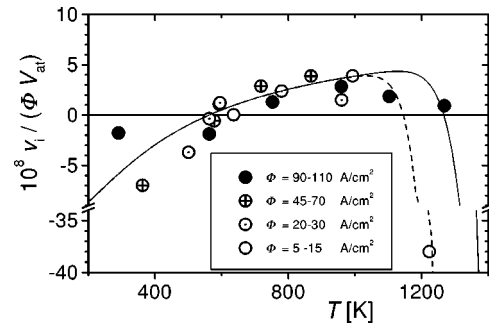


FIG. 7. Scaled velocity of the diamond-graphite transformation as a function of temperature; compilation of data pertaining to irradiation with 1250-keV electrons and irradiation intensities ranging from 5 to 100 A/cm²; full lines: theoretical curves for beam intensities of 5 A/cm² (dashed line) and 100 A/cm² (full line), all other parameters as in Figs. 3–5.

experimentally observed phase transformation velocities was obtained for irradiation with both 400- and 1250-keV electrons in a temperature range from 290 to 1270 K. We note that the relaxation barrier asymmetry ΔG^I deduced from the nonequilibrium phase diagram is of the order of magnitude of the difference in lattice energies of diamond and graphite.¹⁶ Because of this, the qualitative predictions of the earlier paper⁸ remain valid where ΔG^I was implicitly identified with the difference in bulk free energies.

We note that the experimental findings reported in the present paper rule out certain alternative mechanisms for the stabilization of diamond vs graphite under irradiation which have been proposed in the literature:

(i) It has been proposed that during irradiation the higher damage rate in graphite may lead to an accumulation of defects such that the free energy of graphite may be raised above the free energy of diamond.¹⁷ According to this thermodynamic argument, phase stability reversal is expected to prevail at low temperatures where the free-energy difference between graphite and diamond is smallest and damage accumulation in graphite is most efficient. This is clearly inconsistent with our observations: At low temperatures, we find that irradiation actually promotes the transformation of diamond to graphite, while at temperatures where irradiation-induced defects anneal out rapidly and little accumulation of visible damage takes place,¹³ diamond growth is observed.

(ii) A more ‘‘atomistic’’ line of reasoning has been advanced by several authors^{18,19} which point out that during ion deposition, the formation of diamondlike structures may be favored by the fact that under irradiation sp^3 may be more stable than sp^2 sites. The preferential damage of sp^2 sites is, in the present study, reflected by a lower displacement threshold in graphite. This is a necessary condition for irradiation-induced diamond growth, but it is not sufficient to explain all the observations. Additional thermodynamic considerations are required to understand why below a critical temperature irradiation promotes not diamond but graphite growth.

An intrinsic limitation of the experimental method used in the present work stems from the fact that the observations are made on thin film specimens, where surface effects cannot be completely ruled out. In spite of this, the agreement between the experimental observations and predictions of the theoret-

ical model is good. This yields strong evidence for the proposed mechanism of irradiation-induced diamond growth as the result of nonequilibrium processes involving the production and recombination of interstitials at a diamond-graphite interface.

ACKNOWLEDGMENTS

Stimulating discussions with P. Hähner and A. Seeger are gratefully acknowledged. The authors thank R. Höschel for assistance during microscopy.

-
- ¹*The Properties of Natural and Synthetic Diamond*, edited by J.E. Field (Academic Press, London, 1992).
- ²*Properties and Growth of Diamond*, edited by G. Davies (INSPEC, London, 1994).
- ³J.C. Angus and C.C. Hayman, *Science* **241**, 913 (1988).
- ⁴F.P. Bundy, W.A. Bassett, M.S. Weathers, J.R. Hemley, H.K. Mao, and A.F. Goncharov, *Carbon* **34**, 141 (1996).
- ⁵F. Banhart and P.M. Ajayan, *Nature (London)* **382**, 433 (1996).
- ⁶M. Zaiser, in *Microstructural Processes in Irradiated Materials*, edited by S.J. Zinkle, G.E. Lucas, R.C. Ewing, and J.S. Williams, MRS Symposia Proceedings No. 540 (Materials Research Society, Warrendale, PA, 1999), p. 243.
- ⁷F. Banhart, *J. Appl. Phys.* **81**, 3440 (1997).
- ⁸M. Zaiser and F. Banhart, *Phys. Rev. Lett.* **79**, 3680 (1997).
- ⁹Y. Lyutovich and F. Banhart, *Appl. Phys. Lett.* **74**, 659 (1999).
- ¹⁰P. Bellon and G. Martin, *Phys. Rev. B* **38**, 2570 (1988); **39**, 2403 (1989); F. Haider, P. Bellon, and G. Martin, *ibid.* **42**, 8274 (1990).
- ¹¹P.A. Thrower and R.M. Mayer, *Phys. Status Solidi A* **47**, 11 (1978).
- ¹²K. Nakai, C. Kinoshita, and A. Matsunaga, *Ultramicroscopy* **39**, 361 (1991).
- ¹³F. Banhart, T. Füller, Ph. Redlich, and P.M. Ajayan, *Chem. Phys. Lett.* **269**, 349 (1997).
- ¹⁴F. Banhart, *Rep. Prog. Phys.* **62**, 1181 (1999).
- ¹⁵M. Hohenstein, A. Seeger, and W. Sigle, *J. Nucl. Mater.* **169**, 33 (1989).
- ¹⁶*Gmelin Handbook of Inorganic Chemistry* (Springer, Berlin, 1968), Vol. 14 B.
- ¹⁷Y. Bar-Yam and T.D. Moustakas, *Nature (London)* **342**, 786 (1989).
- ¹⁸Y. Lifshitz, S.R. Kasi, and J.W. Rabalais, *Phys. Rev. Lett.* **62**, 1290 (1989).
- ¹⁹H.P. Kaukonen and R.M. Nieminen, *Phys. Rev. Lett.* **68**, 620 (1992).